
COMBUSTION, EXPLOSION,
AND SHOCK WAVES

Propagation of Detonation in Fuel–Air Mixtures in Flat Channels

S. V. Khomik^{a, b, *}, S. P. Medvedev^{a, b}, A. A. Borisov^{b, c}, V. N. Mikhalkin^b, O. G. Maksimova^b,
V. A. Petukhov^a, and A. Yu. Dolgoborodov^a

^a Joint Institute for High Temperatures, Russian Academy of Sciences, Moscow, 125412 Russia

^b Semenov Institute of Chemical Physics, Russian Academy of Sciences, Moscow, 119991 Russia

^c National Research Nuclear University MEPhI, Moscow, 115409 Russia

*e-mail: khomik@chph.ras.ru

Received June 10, 2015

Abstract—The wide scatter of the values of the measured detonation cell size in fuel + air mixtures restricts the applicability of this parameter in the estimation of the geometric limits of detonation propagation, including in rectangular channels whose height is much larger than their width. The critical channel height for the propagation of detonation has been experimentally determined for hydrogen + air, propane + air, and ethylene + air mixtures. In order to reveal the specific features of the propagation and decay of detonation in a narrow channel, numerical simulation has been carried out for a hydrogen + air mixture with account taken of the cellular structure of the detonation wave.

Keywords: detonation, critical propagation conditions, hydrogen, hydrocarbons

DOI: 10.1134/S1990793116020202

INTRODUCTION

The problem of predicting emergency scenarios remains topical because of the increasing use of combustible gases in energy production and in the chemical industry. In addition, there have been persistent attempts to make use of detonation in the limited space of the combustion chambers of various engines. One of the parameters allowing the behavior of a combustible mixture to be predicted is the critical size (cross-sectional area) of the channel through which detonation still can propagate. It was suggested earlier that the critical channel size be estimated using empirical correlations between this parameter and the transverse dimension of the detonation cell, λ . For a cylindrical channel, the critical detonation propagation diameter is approximately λ/π . This relationship has been experimentally verified to within the λ determination uncertainty [1]. In this case, spin detonation propagates in the channel and λ is the transverse dimension of the cell in the stationary detonation wave propagating along the cylindrical channel. The diameter of the channel in which λ is determined should be sufficiently large for the cell size to depend only on the mixture composition and initial pressure. This is typically the case at diameters such that the detonation velocity is diameter-independent. Based on hydraulic analogy for variously shaped channels, Vasil'ev [2] concluded that the critical value of the side length for a square channel is λ/π as well. The cross-sectional area of a rectangular channel is determined by its

width l and height h . At $l/h \gg 1$, the channel can be characterized by its height h alone.

Although the above relationships are suitable for rough estimation of the safe channel size, a more precise determination method, preferably a one that does not involve the parameter λ , is needed for practical applications and for the validation of computational codes. For combustible gas + air mixtures, the λ determination accuracy is not always sufficient for correlation formulas, because detonation has an irregular cellular structure [3]. This circumstance, along with the wide variety of methods of surface preparation for observing triple point trajectories, leads to a wide scatter of measured cell size values. By way of illustration, we show how λ depends on the mixture composition for air + hydrogen and air + propane mixtures (Fig. 1). Figure 1 presents not only experimental data of different authors [4–9] but also data calculated using the model suggested by Gavrikov et al. [10]. Two different kinetic mechanisms, one proposed by Konnov [11] and the other by San Diego [12], were used in these calculations.

For hydrogen + air mixtures, the cell sizes suggested by different authors may vary by a factor of up to 2, which is well above the uncertainty of measuring the cell size for hydrocarbon + air mixtures. Discussion of the cause of this distinction is beyond the scope of this work. In any case, the accuracy of the correlations involving the cell size is not higher than the accuracy of cell size measurements.

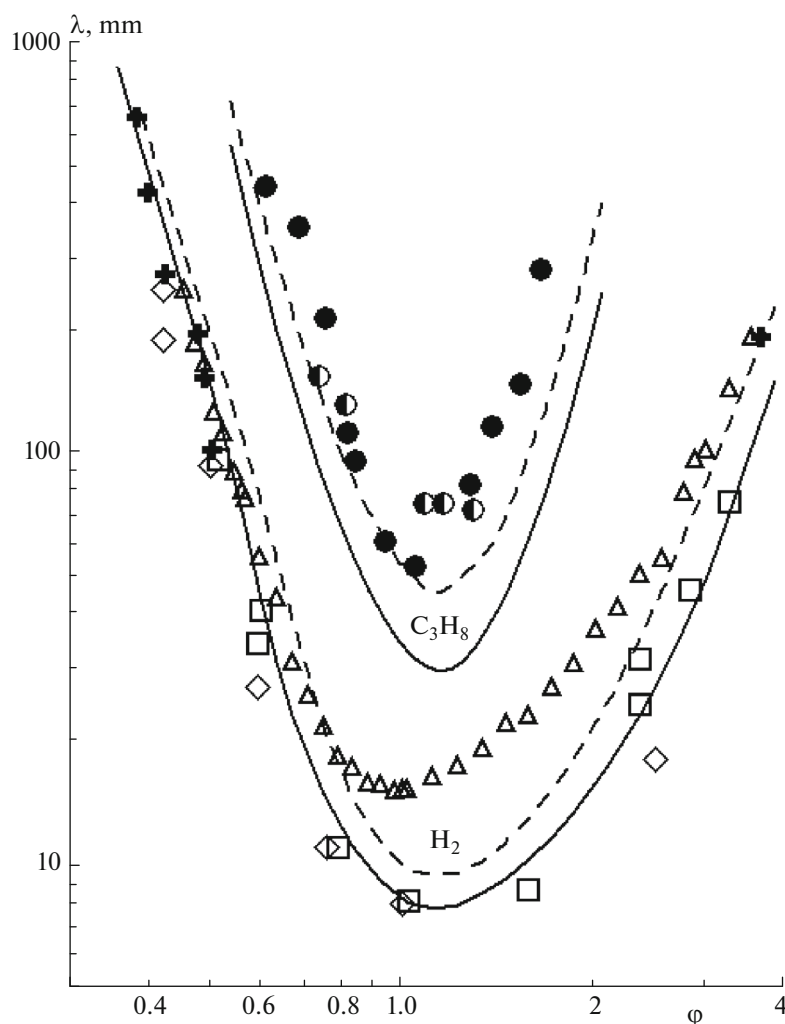


Fig. 1. Detonation cell width as a function of composition for $\text{H}_2 + \text{air}$ and $\text{C}_3\text{H}_8 + \text{air}$ mixtures according to experimental data of different authors (points) and according to the data calculated using the model of Gavrikov et al. [10] with the kinetic scheme suggested by Konnov [11] (dashed curve) and the scheme suggested by San Diego [12] (solid curve): \square [4], \diamond [5], \triangle [6], $+$ [7], \bullet [8], and \circ [9].

The critical channel height h at which detonation propagation is still possible was determined for various mixtures [13–15]. Relative channel dimensions and the cell size were characterized in those works in terms of the λ/h ratio. According to Vasil'ev [13], this ratio is 5–7 for acetylene + oxygen and hydrogen + oxygen mixtures, and according to Monvar et al. [14], it varies between 4 and 8.5 as the detonating gas is diluted with argon. Hydrogen + air and acetylene + air mixtures at a reduced initial pressure (62 kPa) were studied by Weber et al. [15]. They established that detonation in hydrogen + oxygen mixtures decays at $3.7 < \lambda/h < 5.5$. Note that a cell size of 11 mm, measured by the authors themselves [15], was used in that study, although a cell size of 14.3 mm (which is 30% larger) is reported in the literature [16] for the given conditions. It is possible that this difference arises from the specific geometric features of the experiments con-

duced by Weber et al. [15] and is due to the detonation being overdriven in the cell size measurement region. Thus, the accuracy of the correlations between the channel height and the cell size is not high and, moreover, data obtained for fuel + oxygen mixtures cannot be used for fuel + air mixtures. In order to obtain correct estimates and construct numerical models for the development of explosive processes and for detonation propagation in channels, it is necessary to have more precise values of the critical height of the slit. This information can be gained by direct experiments, particularly for hydrogen–air mixtures.

Here, we report an experimental determination of the critical height of a flat channel (slit) along which detonation can propagate in various combustible gas + air mixtures. Limiting pressures were interpreted using the results of two-dimensional numerical simulation. The mixture components were hydrogen, the typical

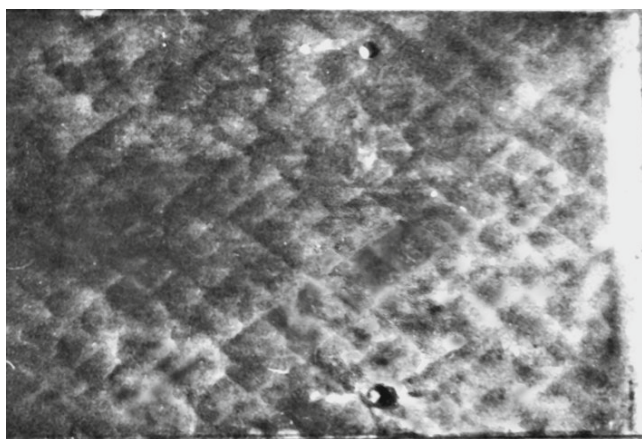


Fig. 2. Detonation of the stoichiometric C_3H_8 + air mixture in a 20-mm-high channel. The detonation wave propagates from left to right. The transverse dimension of the image is equal to the channel width and is 300 mm.

hydrocarbon fuel propane, and ethylene as an example of unsaturated hydrocarbons.

EXPERIMENTAL PROCEDURE AND SUBJECT OF INVESTIGATION

By the experiments described below, we obtained the critical channel heights at which detonation can propagate in the 40% H_2 + 60% air mixture (stoichiometric ratio of $\varphi = 1.59$), stoichiometric C_3H_8 + air mixture, and two C_2H_4 + air mixtures (one stoichiometric and the other lean, with $\varphi = 0.84$). The experiments were carried out in a rectangular channel 1.7 m in length and 0.3 m in width. The channel height was varied between 5.3 and 20 mm using inserts. The narrow sides of the channel were sealed up with a 100- μ m-thick polyethylene film using an adhesive tape. One of the channel ends was also sealed with the film, and a gas mixture inlet manifold was placed there. At the other, open end, we placed a flat plastic explosive charge or a detonating cord, both initiated with a blasting cap. The mixture was prepared in a stirred gas blender and was then blown through the channel to replace the air filling it. The volume of the mixture that was passed through the channel was 5 to 10 times larger than the channel volume. The weight of the initiating explosive charge was approximately 1.5 times larger than the charge weight necessary for initiating the detonation of the gas mixture in a cylindrical channel [17]. For preventing the deformation of the wide plates upon detonation, they were not rigidly fixed. The distance by which the plates were displaced as detonation was propagating along the channel was insignificant. This was ensured by using spring clamps. The light emitted by the detonation front was swept on a rotating photographic film through a slit placed before a film-sealed channel side. Prior to taking measurements, one of the 1.7×0.3 m channel walls was

blackened for obtaining detonation imprints. After the experiment, the detonation imprint was fixed with an aerosol varnish and was then copied on graph paper or photographed. As in an earlier study [18], the transverse dimension of the cell was determined by dividing the channel width in the i th cross section by the number of transverse waves in this cross section that move in the same direction and by averaging the quotient over several cross sections.

EXPERIMENTAL DATA

Processing the observed detonation imprints enabled us to follow the variation of the cell size along the channel length and to determine the multifront detonation cell size averaged over the channel width. Figure 2 shows an imprint observed for the stoichiometric propane + air mixture at a slit height of 20 mm. In this case, the cell size is approximately (60 ± 5) mm.

Figure 3 plots the observed cell size data as a function of the channel length for propane + air and ethylene + air mixtures of different compositions at different channel heights. Clearly, the small cell that appears near the place of initiation owing to a strong overdrive of detonation upon the initiation of detonation with a condensed explosive charge either grows to some constant size, indicating the establishment of a self-sustained propagation regime, or grows throughout the channel length and disappears in some cases.

For example, for the stoichiometric ethylene + air mixture in the 8-mm-high channel, the cell size reaches a constant value of (27 ± 3) mm at a distance of 1.2 m from the initiator, while the cell in the 5.3-mm-high channel reaches a size of 68 mm at the same distance and then disappears. The latter fact indicates the absence of triple-point configurations leaving a detonation imprint that are present in a multifront detonation wave. This is evidence that the detonation wave undergoes degradation (decay). A similar situation is observed for the stoichiometric propane + air mixture. It can be seen in Fig. 3 that, as the channel height for this mixture is decreased from 20 to 17 mm, the distance between the initiating charge and the cross section in which the average cell size becomes invariable, taking a value of (55 ± 5) mm, increases. Further decreasing the channel height to 15 mm causes the decay of the detonation wave, as in the case of the ethylene + air mixture.

Figure 4 presents the results of processing the streak camera records for the propane + air mixture in channels 15 and 17 mm in height. In the former case, the detonation velocity, after showing a quasi-steady-state behavior 0.9–1.0 m away from the initiator, begins to decrease to become 750 m/s at a distance of 1.3 m, where the detonation cell is no longer observed, according to Fig. 3. For the 17-mm-high channel, the detonation velocity takes a value of (1800 ± 100) m/s at a distance as short as 1 m from the initiator. This

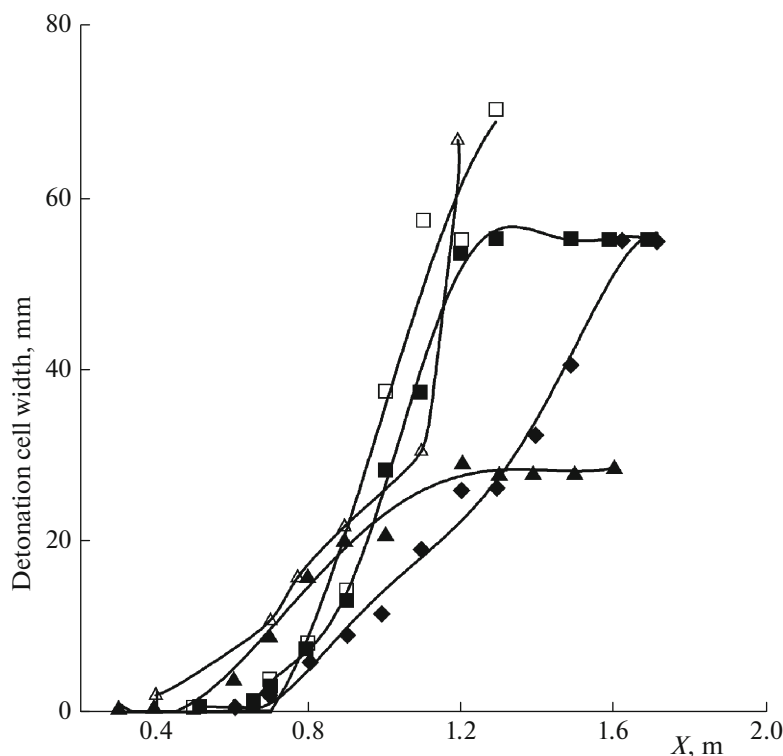


Fig. 3. Variation of the detonation cell width along the length X of the channel. Stoichiometric C_3H_8 + air mixture at a channel height of $h =$ (■) 20, (◆) 17, and (□) 15 mm; stoichiometric C_2H_4 + air mixture at a channel height of $h =$ (▲) 8 and (△) 5.3 mm.

velocity is in satisfactory agreement with the maximum detonation velocity reported for this mixture by other authors [19]. A comparison between Figs. 3 and 4 for the case of propane + air mixture detonation in

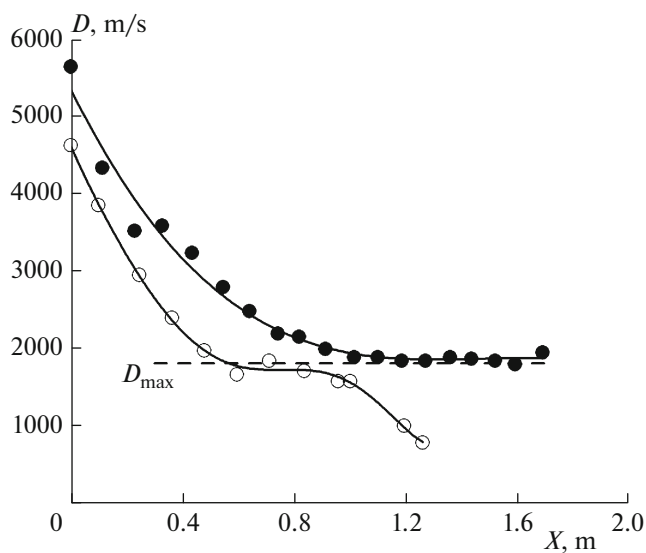


Fig. 4. Variation of the explosive process propagation velocity along the length X of a rectangular channel for the stoichiometric C_3H_8 + air mixture at a channel height of $h =$ (●) 17 and (○) 15 mm.

the 17-mm-high channel demonstrates that, although the detonation velocity is constant at a distance of 1 m from the initiator, the cell size is smaller than its steady-state value, which is reached at a distance of 1.5 m. The same effect was observed for a hydrogen + air mixture [15]. This indicates that the structure and parameters of the detonation wave reach the values corresponding to the self-sustained regime only at a certain distance from the initiator. Therefore, for ascertaining that detonation is stationary, it is necessary to prove the constancy of its spatial structure.

Experiments on the hydrogen + air mixture at $\varphi = 1.59$ demonstrated that detonation propagates in a self-sustained regime at a channel height of $h = 8$ mm, and the cell size in this case was measured to be (24 ± 4) mm. As the channel height was decreased to $h = 6$ mm, the detonation velocity decreased throughout the slit length, indicating a decay of that the detonation wave.

The observed data and the characteristics of the mixtures examined are summarized in the first six columns of the table for detonation propagation (+) and detonation decay (−). The seventh column of the table lists the cell sizes measured in tubes with a rather large diameter [4, 5, 8–10, 20] or calculated using the model suggested by Gavrikov et al. [10]. For the hydrocarbon + air mixtures, these sizes coincide,

Table

Mixture	ϕ	Channel height h , mm	Result	λ , mm (measured)	λ/h	λ , mm (literature)	References	d_{prop} , mm
H ₂ + air	1.59	8	+	24 ± 2	3.0	9 (exp) 10–13 (calc) 23 (exp)	[4, 5] [10] [6]	5 [21]
		6	–		4.0			
C ₃ H ₈ + air	1	17	+	55 ± 5	3.2			
		15	–		3.7			
C ₂ H ₄ + air	1	8	+	27 ± 3	3.4	24 ± 4 (exp)	[8, 20]	n.d.
		5.3	–		5.1			
	0.84	12	+	40 ± 4	3.3	40 ± 4 (exp)	[8, 20]	n.d.
		10	–		4.0			

exp = experimental; calc = calculated; n.d. = no data.

within the measurement error, with the experimental data obtained under near-limit conditions.

For the hydrogen + air mixtures, the discrepancy between our experimental cell size data and the same data available from the literature reaches 100%. If the cell size determined in this study is used for various mixtures, it will be clear that the λ/h ratio lies in the $3 < \lambda/h < 4$ range, differing from the ratio suggested by Vasil'ev [2] in that it indicates a smaller critical channel height. Therefore, the criterion proposed by Vasil'ev [2], which involves the cell size, is suitable only for rough estimation and is inapplicable to hydrogen + air mixtures because of the wide data scatter.

For some mixtures, the critical diameter for detonation propagation in a cylindrical channel, d_{prop} , is known. The table lists these diameters for the stoichiometric hydrogen + air [21] and propane + air [1] mixtures. For the propane + air mixture, the value presented is a lower estimate, because detonation does not propagate at a diameter of 16 mm. The mixture examined in our experiments, 40% H₂ + 60% air, is fuel-rich, and, according to the data presented in Fig. 1, its sensitivity is lower than the sensitivity of the stoichiometric mixture. It would, therefore, be expected that the critical diameter for detonation propagation in a cylindrical channel for the rich mixture will fall in the 6–8 mm range, like the critical height of the flat channel. Thus, this study quantitatively verified the qualitative conclusion that the critical channel height is equal to the critical diameter for detonation propagation, without involving the detonation cell size, a parameter that is inaccurately determined for mixtures with an irregular structure. Because of this fact, both rather rough correlations and directly measured critical detonation propagation heights and diameters can be used in practice, depending on the purpose in hand.

RESULTS OF NUMERICAL SIMULATION

Numerical simulation of the initiation, propagation, and decay of a detonation wave provides means to reveal the parameters and regularities of fast physicochemical processes that are experimentally undeterminable in many cases. The increase in computing power and the development of numerical methods in recent years have made it possible to successfully interpret experimental data in some problems associated with gas detonation. However, the practically important problem of calculating the limits of propagation of a detonation wave in narrow channels and slits has not been solved to date. It was noted in a recent work [22] that present-day approaches are based on application of numerical methods to development of ideas that were put forward in classical studies [23, 24]. Although the models presented in those studies are physically clear and well-substantiated, certain assumptions concerning the flow pattern have to be made for performing numerical simulations. For this reason, it was concluded [22] that there is no quantitative theory capable of predicting the geometrical limits of detonation. Without casting doubt on this conclusion, we will note that the results of numerical simulation associated with particular experimental data can be of some use in elucidation of the mechanisms of detonation propagation regimes and decay conditions.

Using the hydrogen + air mixture as an example, we will consider the possibility of applying a standard procedure for solving gas dynamics equations to numerical simulation of the propagation of a detonation wave in a narrow slit and to interpretation of experimental data. The calculations were carried out using the gas dynamics simulation software Gas Dynamics Tool (GDT) [25]. This software was used earlier to numerically solve gas dynamics and chemical kinetics equations in an analysis of the interaction of detonation and shock waves with permeable barriers

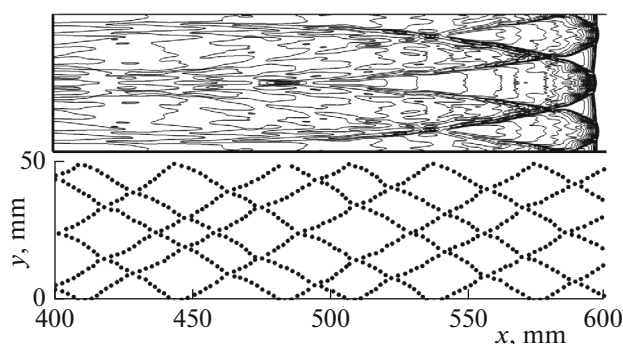


Fig. 5. Calculated pressure isolines (line spacing, 0.1 MPa) and cellular detonation wave structure for the 40% H₂ + 60% air mixture at $p = 0.1$ MPa and $T = 293$ K.

[26–28]. The GDT software, using the modified large-particle method, solves Navier–Stokes equations, taking into account transfer processes and heat evolution as a result of a chemical reaction. It is assumed that the gas is viscous and heat-conducting, with a heat capacity ratio of $\gamma = 1.35$. The rate of the overall Fuel + Oxidizer \rightarrow Products reaction is an Arrhenius-type function of temperature involving the relative mass concentrations of fuel [F] and oxidizer [O]:

$$k = A[F]^n[O]^m \exp\left(-\frac{T_a}{T}\right). \quad (1)$$

The parameters in Eq. (1) were set with account taken of self-ignition delay data calculated for the mixture examined from a detailed reaction mechanism. For the object of our study—40% H₂ + 60% air mixture—the activation energy under normal conditions is $T_a = 11\,000$ K, $A = 3 \times 10^{13}$ 1/s, $n = 1$, and $m = 8$. The values of viscosity, thermal conductivity, and diffusion coefficient were calculated using the GASEQ software package [29]. Simulation was carried out for a two-dimensional problem formulation on a rectangular and nonadaptive mesh with a cell size of 0.2 mm.

The calculations were carried out in two steps. In the first step, we elucidated the flow pattern for the propagation of multifront detonation in a 50×1000 mm channel. For the initiation of a detonation wave at the left boundary of the computational region, we set an increased temperature and pressure in a 1-mm-thick layer. As the detonation wave was propagating in the channel, instabilities (perturbations of gas dynamic parameters) developed at its initially smooth front and a cellular detonation wave structure formed already 0.4 m away from the initiator. The pressure isolines at the top of Fig. 5 illustrate the flow pattern in the channel at a distance of about 0.6 m from the initiator, showing a system of frontal triple-point configurations characteristic of detonation.

At the bottom of Fig. 5, one can see the trajectories of local pressure maxima (triple points) simulating the irregular cellular structure of detonation. The trans-

verse dimension of the cells varies between 12 and 22 mm, within the scatter of experimental data for the 40% H₂ + 60% air mixture under normal conditions. Thus, although a simplified, two-dimensional approach was used, the results of numerical simulation are in agreement with data available both on the detonation cell size and on the average detonation front velocity that is close to the Chapman–Jouguet detonation velocity $D_{CJ} = 2100$ m/s.

The calculated data obtained in the first step form an array of boundary conditions for the problem of detonation wave propagation in a two-dimensional channel (slit) whose height is smaller than the detonation cell size. According to experimental data for the 40% H₂ + 60% air mixture, detonation does not propagate at $h = 6$ mm (see the table). This value was used in the main series of explosion mode calculations using an elongated, 6×5000 mm computational region. The left-hand side boundary conditions (at the channel inlet) were set (in tabular form) as the time dependences of pressure, density, and two gas (combustion products) velocity components calculated in the first step for the $x = 500$ mm cross section at $y = 0$ to 6 mm. It was verified by a special-purpose series of calculations that this technique actually simulates the entry of a multifront detonation wave into a narrow channel without perturbations caused in the inlet region by reflection from the channel walls. The simulation was aimed at reconstructing a detonation wave decay regime that is in agreement with experimental data.

For correctly describing the gas flow in narrow channels at large Reynolds numbers, it is necessary to take into account turbulization behind the wave front [23]. The calculated cell size, which is 0.2 mm, is too large for a detailed resolution of the turbulent eddy structure. In this situation, it is pertinent to take into consideration the turbulence effect by substituting effective, much larger, “turbulent” transfer coefficients into the equations being solved, as was done by other authors [30, 31]. To simplify the analysis, the viscosity, thermal conductivity, and diffusion coefficient in the calculations were varied by multiplying them by a correction factor K and the Schmidt and Prandtl numbers were fixed. The results of these calculations are presented in Fig. 6 as the lead shock wave front velocity versus the distance traveled. As was expected, the calculation using standard tabulated molecular transfer coefficients (curve 1) did not reveal any tendency to the decay of the explosive wave, which propagated at a velocity close to D_{CJ} up to a distance of 5 m from the initiator. Increasing the parameter K led to a decrease in (lack of) the explosive process velocity, just as was observed in experiments. A dramatic change in the character of explosion took place as K was increased from 96 to 97. At $K = 96$ (Fig. 6, curve 2), an explosive regime propagated in the channel at a constant mean velocity of about 1750 m/s. After the

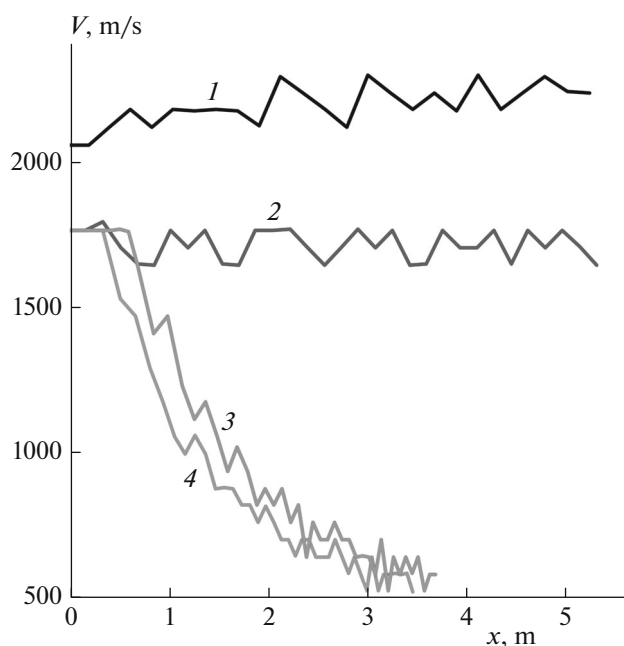


Fig. 6. Calculated lead shock front velocity as a function of the distance from the initiator at different values of the correction factor: $K = (1)$ 1, (2) 96, (3) 97, and (4) 100. The velocity averaging interval is 100 μ s.

correction factor was slightly increased to $K = 97$ (curve 3), the velocity of the lead shock wave began to decrease at a distance of about 0.9 m and eventually fell down to approximately 600 m/s. As K was further increased, the wave decay onset coordinate shifted to the place of initiation ($K = 100$, curve 4).

In order to elucidate the details of explosive process propagation under limiting conditions ($K = 97$), it is of use to analyze the flow pattern frame by frame at various distance from the initiator. Figure 7 presents the results of calculation in the form of pressure isolines superposed with the region occupied by the combustion products. As can be seen in Figs. 7a and 7b, the lead shock wave and the reaction front undergo visible separation in the initial region of the channel. The quasi-steady-state region in which explosive process propagates at a velocity of about 1750 m/s is illustrated in Fig. 7c, from which it follows that ignition takes place in a transverse wave that is alternately reflected by the upper and lower boundary planes. Note that, for maintaining the intensity of the transverse wave, it is necessary that ignition occur before the next reflection. A flow pattern similar to that shown in Fig. 7c takes place under subcritical conditions at $K = 96$, and in this case it persists up to the end of the computational region ($x = 5$ m). At $K = 97$, the momentum

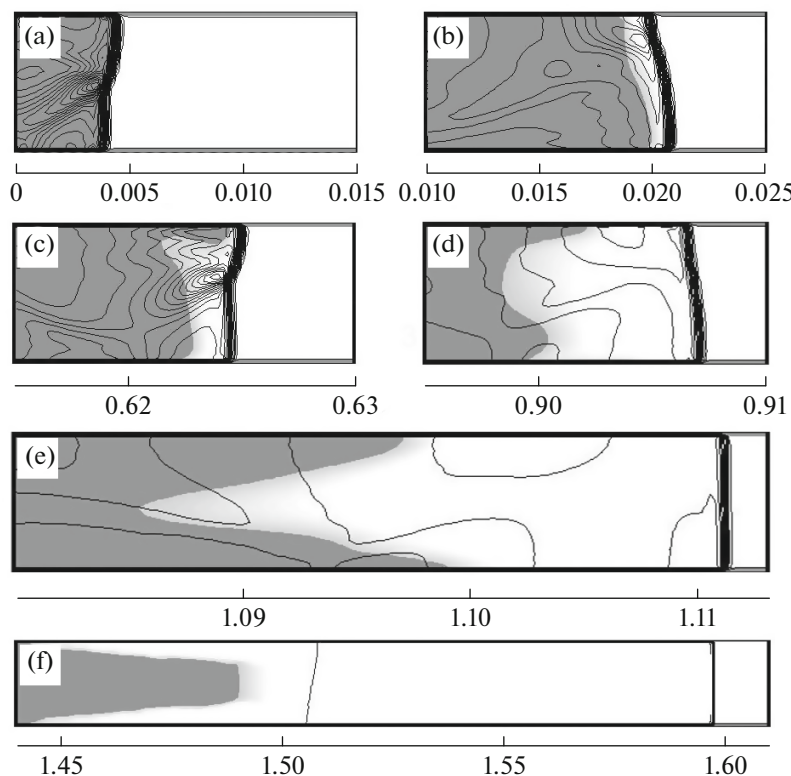


Fig. 7. Calculated pressure isolines (line spacing, 0.1 MPa) together with the regions occupied by the combustion products. The distances are in meters.

losses weaken the transverse wave and, accordingly, lead to a progressive increase in the ignition delay time. The distance between the front of the lead shock wave and the visible reaction front increases, and the transverse wave undergoes blurring, as is demonstrated in Fig. 7d. As the explosive process intensity decreases further, a reversal of the shape of the reaction front takes place (Figs. 7e, 7f).

Thus, despite the simplifications made, the above analysis demonstrates that a promising way of interpreting the limit phenomena in detonation of propagation in slitlike channels is by taking into account the turbulence effect through the introduction of effective transfer coefficients. On the one hand, this approach makes it possible to perform multidimensional calculations on relatively coarse meshes; on the other hand, it allows experimentally observed effects to be reproduced. The maximum calculated detonation velocity deficiency is about 17%, which is in agreement with experimental data. An analysis of the results of two-dimensional simulation demonstrates that the detonation propagation limit for a flat channel is due to the weakening of the transverse wave.

ACKNOWLEDGMENTS

Experimental studies were supported by the Russian Science Foundation (project no. 14-50-00124) and were carried out at the Joint Institute for High Temperatures, Russian Academy of Sciences. Numerical simulation was supported by the Rosatom State Nuclear Energy Corporation (state contract no. N.4kh.44.90.13.1106) and was carried out at the Semenov Institute of Chemical Physics, Russian Academy of Sciences. Photographic sweeps were processed at the Department of Chemical Physics, National Research Nuclear University MPhI.

REFERENCES

1. A. A. Borisov, B. E. Gel'fand, S. A. Loban', A. E. Maiklov, and S. V. Khomik, *Khim. Fiz.*, No. 6, 848 (1982).
2. A. A. Vasil'ev, *Fiz. Goreniya Vzryva* **23** (3), 121 (1987).
3. V. V. Mitrofanov, *Detonation of Homogeneous and Heterogeneous Systems* (Inst. Gidrodinam. im. M. A. Lavrent'eva, Novosibirsk, 2003) [in Russian].
4. G. Ciccarelli, T. Ginsberg, J. Boccio, et al., *Combust. Flame* **99** (2), 12 (1994).
5. G. Ciccarelli, T. Ginsberg, J. Boccio, et al., BNL Report No. NUREG/CR-6391, BNL-NUREG-52482 (1997).
6. C. M. Guirao, R. Knystautas, J. Lee, W. Benedick, et al., in *Proceedings of the 19th International Symposium*

7. S. R. Tieszen, M. P. Sherman, W. B. Benedick, et al., *Prog. Astronaut. Aeronaut.* **106**, 205 (1986).
8. R. Knystautas, C. Guirao, J. H. S. Lee, et al., *Prog. Astronaut. Aeronaut.* **94**, 23 (1984).
9. I. O. Moen, J. W. Funk, S. A. Ward, et al., *Prog. Astronaut. Aeronaut.* **94**, 55 (1984).
10. A. I. Gavrikov, A. A. Efimenko, and S. B. Dorofeev, *Combust. Flame* **120**, 19 (2000).
11. A. A. Konnov, <http://homepages.vub.ac.be/~akonnov/>. Cited 2000.
12. <http://maemail.ucsd.edu/~combustion/cermech/>. Cited 2003.
13. A. A. Vasil'ev, *Fiz. Goreniya Vzryva* **18** (2), 132 (1982).
14. M. Monvar, Y. Yamamoto, K. Ishii, et al., *J. Thermal Sci.* **16**, 283 (2007).
15. M. Weber, H. Olivier, and H. Grönig, in *Proceedings of the 23th ISSW* (2001), CD-ROM, Paper 1312, p. 173.
16. D. W. Stamps and S. R. Tieszen, *Combust. Flame* **83**, 353 (1991).
17. A. A. Borisov, S. V. Khomik, V. N. Mikhalkin, et al., *Prog. Astronaut. Aeronaut.* **133**, 142 (1989).
18. N. V. Bannikov and A. A. Vasil'ev, *Fiz. Goreniya Vzryva* **19**, 164 (1993).
19. A. A. Borisov and S. A. Loban', *Fiz. Goreniya Vzryva* **13**, 729 (1977).
20. S. B. Murray and J. H. Lee, *Prog. Astronaut. Aeronaut.* **94**, 80 (1984).
21. D. Pawel, H. Vasatko, and H. Gg. Wagner, AFOSR 69-2095 TR (1969), p. 60.
22. A. Camargo, H. D. Ng, J. Chao, et al., *Shock Waves* **20**, 499 (2010).
23. Ya. B. Zel'dovich, *Zh. Eksp. Teor. Fiz.* **10**, 542 (1940).
24. J. A. Fay, *Phys. Fluids* **2**, 283 (1959).
25. A. V. Zibarov, D. M. Babaev, and A. M. Shadskii, *SAPR Grafika*, No. 10, 44 (2000).
26. S. P. Medvedev, S. P. Khomik, and B. E. Gel'fand, *Russ. J. Phys. Chem. B* **3**, 963 (2009).
27. O. G. Maksimova, S. P. Medvedev, S. V. Khomik, et al., in *Combustion and Explosion*, Ed. by S. M. Frolov (Torus, Moscow, 2012), No. 5, p. 125 [in Russian].
28. S. V. Khomik, S. P. Medvedev, B. Veyssiere, H. Olivier, O. G. Maximova, and M. V. Silnikov, *Russ. Chem. Bull.* **63**, 1666 (2014).
29. *Gas Equation Software Package*, Vers. 0.79 (ChrisMorley, 2005). <http://www.gaseq.co.uk/>
30. V. A. Gal'burt, M. F. Ivanov, V. N. Mineev, et al., *Mat. Model.* **14** (1), 73 (2002).
31. H. D. Ng, J. Chao, and J. H. S. Lee, in *Proceedings of the 20th ICDERS* (McGill Univ., Montreal, Canada, 2005), CD-ROM, Paper 184.

Translated by D. Zvukov